DFT and TD-DFT investigation of calix[4]arene interactions with TFSI– ion

B. Gassoumi, H. Ghalla, R. Ben. Chaabane

DFT and TD-DFT investigation of calix[4]arene interactions with $TFSI^-$ ion

B. Gassoumi[1,3], H. Ghalla[2], R. Ben. Chaabane[1]

[1]*Laboratory of Advanced Materials and Interfaces (LIMA), University of Monastir, Faculty of Science of Monastir, Avenue of Environnment, 5000 Monastir, Tunisia.*

[2]*University of Monastir, Quantum Physics Laboratory, Faculty of Science, Monastir 5079, Tunisia.*

[3]*Institute of Light and Matter, UMR5306 University of Lyon 1-CNRS, University of Lyon, 69622 Villeurbanne cedex, France.*

Abstract

Understanding the interactions of the calix[n]arene molecules with a variety of invited chemicals entities is getting very important. In this context, we have studied a new host-guest such as the interaction of the calix[4]arenes with the bis (trifluoromethylsulfonyl) imide $TFSI^-$ ion. The energy gap has decreased from 3.53 eV to 2.11 eV indicating the reliability of the electrochemical evaluation of HOMO and LUMO energy levels. In a predominant number of cases, we obtain the spatial accumulation of HOMO and LUMO at the interface of phenol groups. Then, according to the Q_{NBO} charge distribution of these host-guests interactions, we have demonstrated the direction of charge transfer between the CX[4] molecule and the $TFSI^-$ ion. More importantly, the non covalent interactions (NCI) have been investigated that the endo-cavity position of the $TFSI^-$4 is the most stable position between all these host-guests. By using DFT quantum methods, we have identified as a suitable host for $TFSI^-$ which can be used in the electronic technology.

Keywords: Calix[n]arene, $TFSI^-$ ion, electronic properties, gap energy, TD-DFT, Non covalent interactions.

1. Introductions

The calix[n]arenes (abbreviated as CX[n]) are macro-molecules based on the phenol groups with a special cavity to encapsulate chemicals entities. The selective admission of the invited molecules in the macro or microscopic systems facilitates the recognition of the electrostatic and magnetic properties of the several cationic or anionic guests [1-5]. In this context, the CX[4] have been chosen in our study because of their own chemical composition and the

* Corresponding author

Email address: gassoumibouzid2016@gmail.com (B. Gassoumi)

hydrophobic cavity form [6]. This chemical material synthesized by a specific diameter and height, which facilitates the interactions with the diversity of the chemical species (cationic, anionic or neutral guests) and small molecules [7, 8, 9]. Recently, these molecules and especially their own cavity entice the researchers of those adaptations with most of the materials to be functional in the medical [10-12] or microbiological field [13, 14]. Also, these molecules are used in the activation of the solubility of monomers in the specific media and in the pharmaceutical drug delivery. Surrounding this strategy, we have explored the photo-physical properties of the complexes CX[4]-$TFSI^-$ (endo-cavity and exo-cavity position of the $TFSI^-$ ion). By using the DFT calculations, we have described the dynamic stabilities of the CX[4]-$TFSI^-$ (CX[4]-T) complexes. The electronic properties have explained the phenomenal rigidity and conductivity of each host-guest. The recognition of the weak or the strong and the nature of the interactions of such guest with the CX[4] molecule have been analyzed by the non-covalent RDG function.

2. Computational detail

The stable structures of the CX[4]-$TFSI^-$ complexes have been optimized with the DFT method by using the global hybrid Generalized Gradient Approximation (GGA) functional B3LYP [15, 16, 17]. This method together with the empirical Becke and Johnson damping dispersion corrections D3BJ in combination with the 6-31+G(d) basis set [18,19] is implemented in Gaussian 09 program [20] and Gauss View [21] as a visual program. The binding energies of CX[4]-$TFSI^-$ complexes are calculated including the BSSE (Basis Set Superposition Error) counterpoise (CP) corrected energy of Boys and Bernardi [22], which considers the fragments relaxation terms and the changes of the conformations in such geometric form. The binding energies are given by the following formula:

$$\Delta E_{CX[4]\text{-}TFSI^-} = E_{CX[4]\text{-}TFSI^-} - E_{CX[4]} - E_{TFSI^-} + BSSE$$

where $E_{CX[4]}$, E_{TFSI^-}, and $E_{CX[4]\text{-}TFSI^-}$ are the total energies of the host and the guest or the host-guest molecules.

The absorption spectra of the CX[4]-$TFSI^-$ complexes have been calculated using TD-DFT method at CAM-B3LYP-D3/6-31+G(d) level. In this part, there are explanations in depth for the variation of the wavelengths of an endo-complex towards another exo-complex. The electronic study of the calixarene-$TFSI^-$ complexes are very effective to show the specificity of each invitation to these materials. The stabilization energies and intermolecular interactions of CX4-$TFSI^-$ complexes have been stimulated at the same theoretical framework. Molecular orbital analysis has been studied to explain the variation of the gap energy and the electron

delocalization passing from $TFSI^-1$ to $TFSI^-4$. The study of the type of the interaction between the calixarene molecule and $TFSI^-$ ion is better explained using the non-covalent interaction-reduced density gradient (NCI-RDG). The NCI-RDG [23] analysis presents the graphical visualization of the non-covalent interaction regions in real-space, distinguishing hydrogen bonds and determining of the Van der Waals or repulsive interactions using simple color codes. The charge transfer has been also studied theoretically between the CX[4] molecule and the $TFSI^-$ ion by the NBO analysis.

3. Calix[n]arene–$TFSI^-$ complexes investigate by DFT method

3.1. Stable geometries and Adsorption energy analysis

The development of encapsulation for the cyclic macromolecules such as β-Cyclodextrine, Cucurbit[n]urils and calixarenes is very effective to find the best host-guest suitable for the applications in the very intersect fields (technological [24] or vital [25, 26]). In this category, we have encapsulated the calix[4]arene molecules by the $TFSI^-$ ion. We have optimized all the structures at the B3LYP-D3/6-31+G(d) level of theory. Moreover, we discussed our results for the CX [4]-$TFSI^-$ complexes based on the position of $TFSI^-$ion. The computational study indicates that the CX4-$TFSI^-$ possesses 4 host-guests (See Figure1), their binding energies are illustrated in Table 1. We have calculated the binding energy of the supra-molecular complexes such as the bis(trifluoromethanesulfonyl)imide ($TFSI^-$) molecules located at the endo-cavity position inner of the phenol ring, the ionic molecule located in the exo-cavity position such as the fluorine branch directed to the center of the cavity, the $TFSI^-$ion located between the two phenolic branches outside the cavity. In this position, these molecules are well balanced by the hydrogen bonds. This molecule has been located outside the cavity such as the oxygen atom directed to the lower edge level. The optimization of the CX[4]-$TFSI^-1$ gives a binding energy value equal to 52.23kcal/mol. The no-destruction of the OH network ensures the conservation of the C_4 symmetry group in this material. Moreover, the energy of the CX[4]-$TFSI^-2$ (endo-cavity) is higher than the first supra-molecular complex, this value is equal to 52.090kcal/mol. The stability of this complex is due to the interaction of the fluorine atoms with the cyclic network of the hydrogen bonds. Moreover, the interaction of this fluorine extremity with the hydrogen atoms connected to the phenol groups promotes the stability of this material.

Table 1: Binding energy of CX[4]-$TFSI^-$ complexes

Complexes	E_b	BSSE	E_b (with BSSE)
CX4-$TFSI^-$1	54,23	0.0028	52.23
CX4-$TFSI^-$2	52.09	0.0020	52.09
CX4-$TFSI^-$3	36.09	0.0046	36.09
CX4-$TFSI^-$4	53.28	0.0022	53.28

The weak electrostatic interaction of the $TFSI^-$ ion with the macro-cycle molecule leaves this complex placed third considering the stabilization order in comparison with others complexes. The complex CX[4]-$TFSI^-$3 has a lower value of the binding energy in comparison with CX[4]-$TFSI^-$2 and CX[4]-$TFSI^-$1. The value of adsorption energy is equal to 36.09kcal/mol. The interaction of the hydrogen bonds of the two oxygen atoms connected to the sulfur atoms ensures the stability of this chemical compound. We note that, the interaction of the H-phenyl rings and the oxygen-fluorine groups was forming the weak CH—π hydrogen bonding. The complex CX[4]-$TFSI^-$4 is the most stable system among all the other host-guests. The binding energy in this chemical material is around to 53.28kcal/mol. The stability of this structure is due to the interaction of oxygen atom connected to the sulfur atom with the hydrogen OH bond located at the lower edge levels. The larger stability of this complex is due to the dipole-dipole interaction between the $TFSI^-$4 ion and the calixarene molecule. This interaction promotes the reduction of the symmetry groups from C_4 to the C_1.

Top views	Bottom views
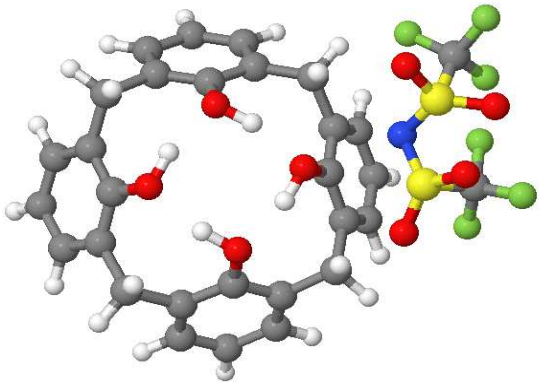	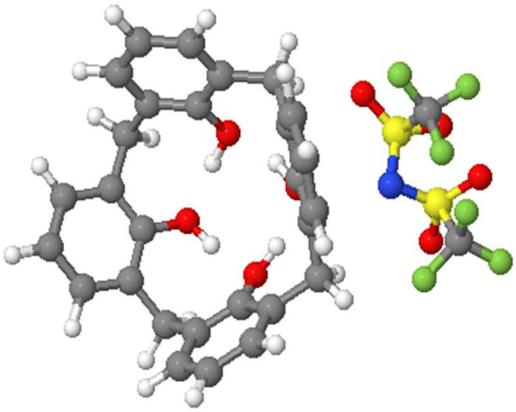
(a)	
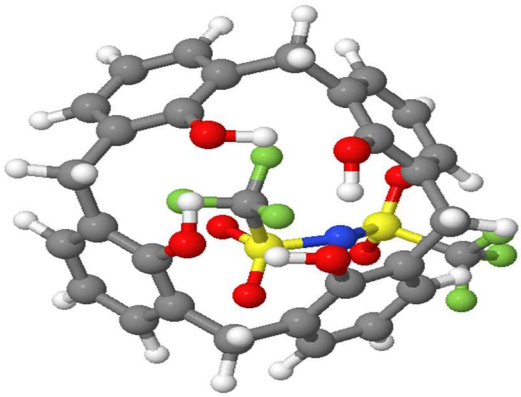	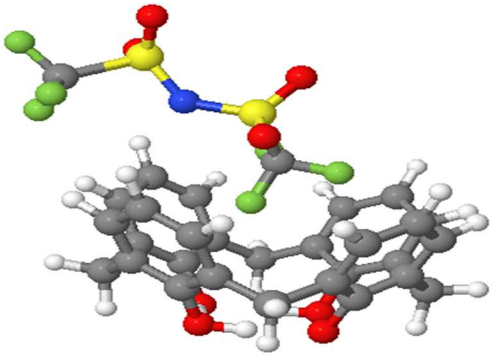
(b)	
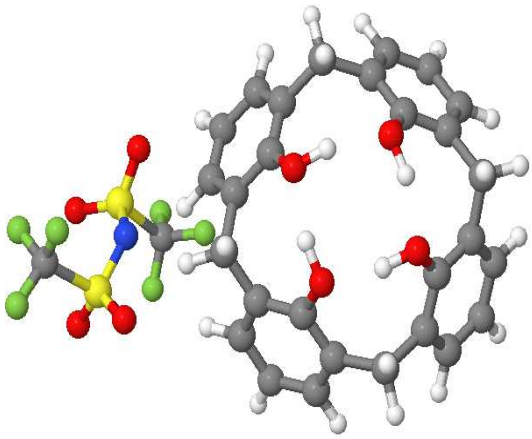	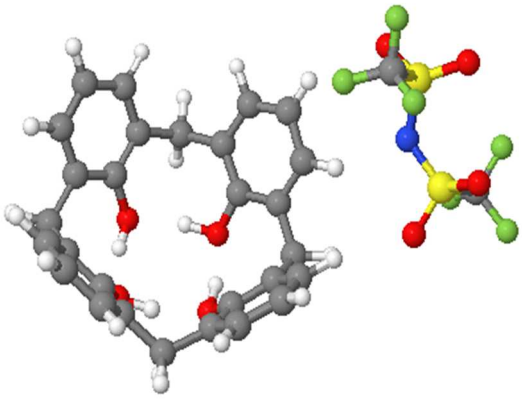
(c)	

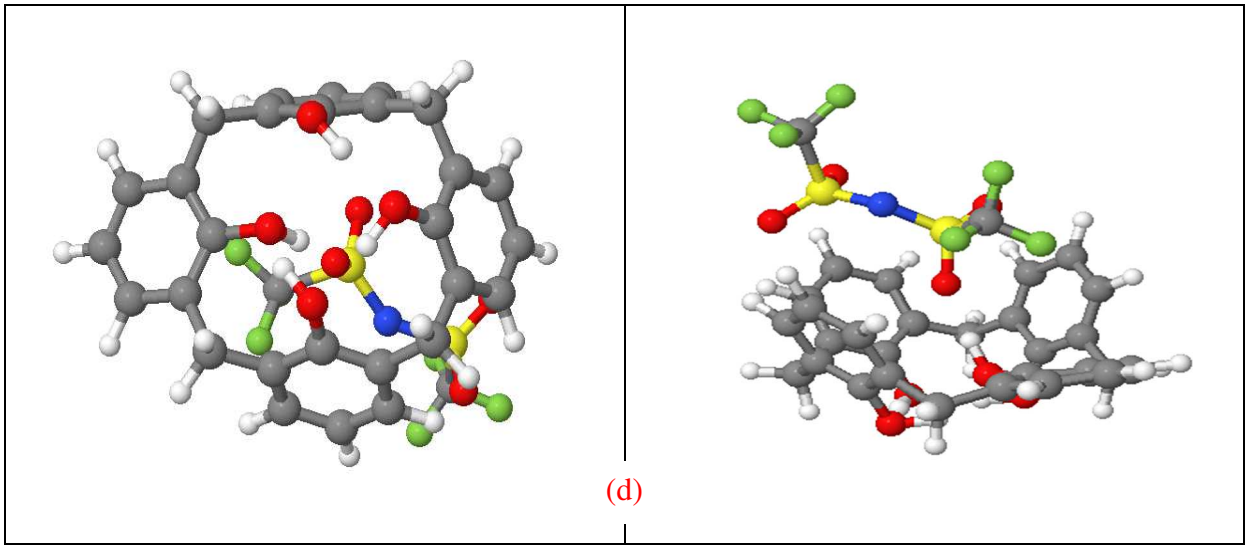

Figure 1. Optimized geometries of and CX[4]-TFSI$^-$ (CX[4]-TFSI$^-$1 (a), CX[4]-TFSI$^-$2 (b), CX[4]-TFSI$^-$3 (c), CX[4]-TFSI$^-$4 (d)) (Top views and Bottom views) structures using B3LYP-D3/6-31+G(d) method.

3.2. Electronic absorption spectra

UV-visible spectrum of the four supra-molecules complexes will be studied to understand the electronic behavior of the different host-guests. Figure 2 shows the superposition of the absorption spectra in the order of stability for these chemical compounds. From these spectra, we have found that the CX[4]-T complexes have an effective wavelength λ in the vicinity of 246 nm for the complexes CX[4]-T4, T2 and 244 nm, 243 nm for the CX[4]-T1 and CX[4]-T3 molecules successively. In this region we can deduce that the complex CX[4]-T2 has a more intense peak in comparison with the other supra-molecular complexes. The red-shifted of the wavelengths λ in the spectrum CX[4]-TFSI$^-$2 is explained as, this molecule has a high sensibility to the calixarene molecules and a lower excited state than other host-guests. The TD-DFT computation for the interest complexes predicts a strong electronic transitions located at 256 nm corresponding to the CX[4]-T4. Figure 2 shows the S0 to S1 transition of the four endo-VS-exo cavity complexes located near the 220, 221, 219 and 218 successively. The different wavelengths λ of the three most stable complexes is almost 1 or 2 nm. This region is characterized by the population of electronic charges surrounding the phenol groups located in the front of the invited ion. In addition, we notice, the appearance of the three corrective peaks having an important intensity in the neighborhood of 202 nm for the CX[4]-

T1/T2 complexes and 198 nm for the CX[4]-T3 complex. In this zone there is a regrouping of electron charges in the region of the interaction between the invited and the calix[4]arene molecule.

Table 2: Main transition states, the corresponding assignments, Eg and oscillator strength, for all compounds, recorded with TD-DFT/CAM-B3LYP/6-31+G(d) method.

Compounds	Electronic Transitions	Energy gap (eV)	Oscillator strength(f)	Molecular orbital
$TFSI^-1$	S0 ⟶ S1	2.83	0.2968	H ⟶ L+2
$TFSI^-2$	S0 ⟶ S1	2.95	0.2376	H ⟶ L+3
$TFSI^-3$	S0 ⟶ S1	3.53	0.4747	H ⟶ L+1
$TFSI^-4$	S0 ⟶ S1	2.11	0.2986	H ⟶ L+5

The π to π^* transitions were expected to co-exist at the low wavelength λ levels near to 189 nm for CX[4]-T1/T3/T4 and 187 nm for CX[4]-T2. These transitions may be due to the interaction of the aromaticity of the phenol group with the organic compound. Finally, the supra-molecular complexes CX[4]-T2/T3 have two low red-shifted peaks located in the vicinity of 182 nm. Concerning the CX[4]-T2 complex, this peak may be due to the presence of the electronic charges at the center of the cavity linked to the existence of the H-bonding between the Host and the guest. In the same framework, the CX[4]-T3 complex is specified by the maximum electronic charges in the region of interactions between the fluorine group and the OH group of the CX[4] molecule.

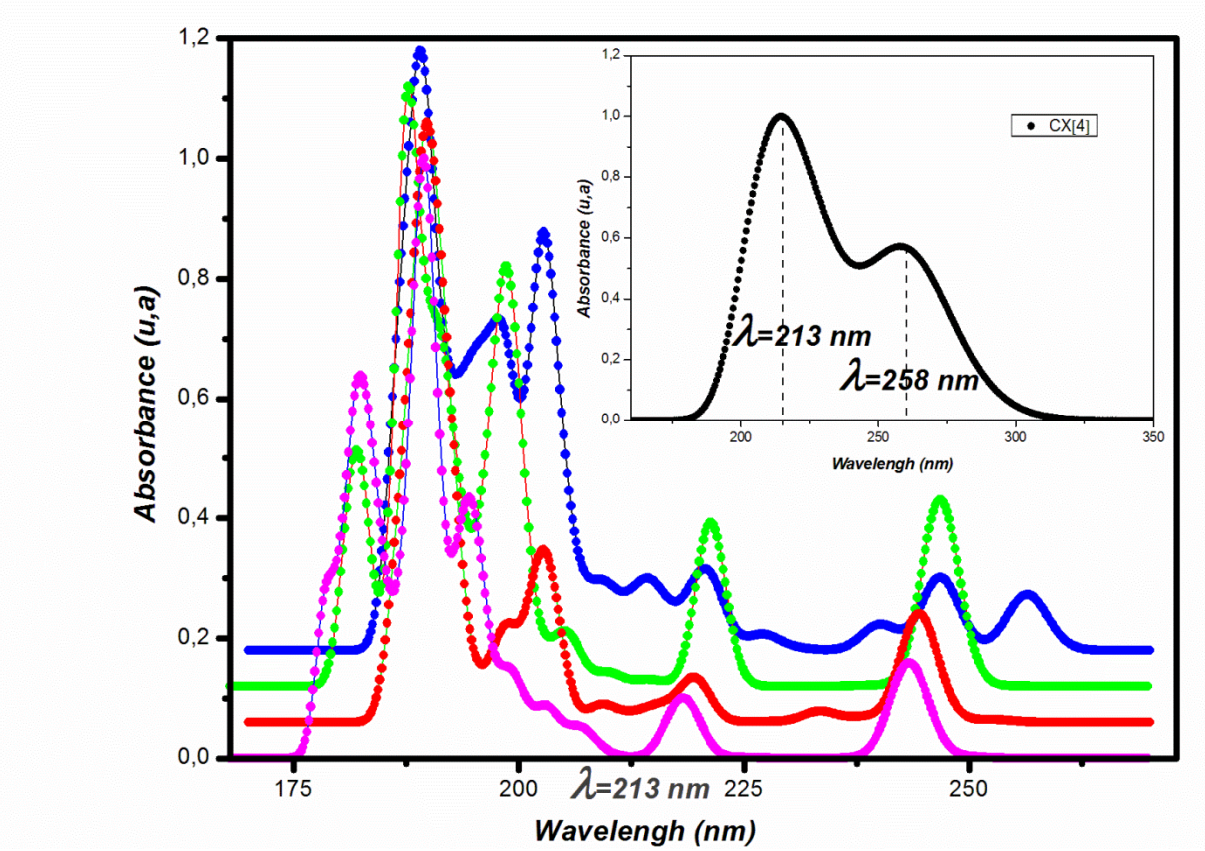

Figure 2. Absorption spectrum of caption of $TFSI^-$ ion by calix[4]arene molecule (Blue: CX[4]-$TFSI^-$4, Green: CX[4]-$TFSI^-$2, Red: CX[4]-$TFSI^-$1, Magenta: CX[4]-$TFSI^-$3) (according to the order of stability).

3.3. FMO study

The ability to donate an electron; HOMO and the ability to accept an electron; LUMO is a very interesting study to take into account the chemical stability part of these macro-cycle complexes. The energy gap (E_g) is an important parameter which explains the chemical stability of these organic compounds very well. In Figure 3, we have depicted the Frontier Molecular Occupied HOMO and the Frontier Molecular Unoccupied LUMO+1, LUMO+2, LUMO+3 and LUMO+5 of CX[4]-$TFSI^-$T1/T2/T3/T4. We have calculated all these FMO at the TD-CAM-B3LYP-D3/6-31+G(d) level of theory. From Figure 3, we can see that, the occupied frontier specified by the red color, or the unoccupied frontier specified by the blue color. The HOMO-LUMO energy gaps of the four stable complexes are equal to 3.53eV (f=0.4747), 2.95eV (f=0.2376), 2.83eV (f=0.2968) and 2.11eV (f=0.2986) successively. According to Figure 3, we find that, it's very clear that the HOMO orbital of the CX[4]-T2/T3 is well delocalized and present at the levels of the cyclic phenol group. The majority of the charge population in the CX[4]-T3 complex co-exists in the phenol groups located in the front of $TFSI^-$ ion. Concerning the second host-guest, we show that, the maximum of the charge

distribution is located around the $TFSI^-$ molecule. The region in the front of the guest has a low delocalization. On the contrary, the organic compound CX[4]-T4 is characterized by a delocalized frontier orbital located on the levels of the phenol group aromaticity near the $TFSI^-$ ion. The FMO L+1/2/3/5 of these chemical compounds are characterized by unequal charge distributions at the phenol group levels in the region of CX[4]-$TFSI^-$ interaction. The complex CX[4]-$TFSI^-$1 is characterized by an electronic delocalization situated in the symmetrical phenol groups. The π-binding orbital LUMO+3 of the CX[4]-$TFSI^-$2 is characterized by an important population of the charge distributions. The population of the charge delocalized of the CX[4]-$TFSI^-$2 complex is located in all symmetrical phenol groups. The complex CX[4]-$TFSI^-$3 has a π-electronic charge located at the phenol group in front of the invited molecule. The unoccupied molecular orbital LUMO+1is specified by the existence of a maximum electronic population located around the two phenol groups in the face of the invited molecule. Moreover, from Table 2 we can deduce that, the CX[4]-$TFSI^-$4 is very conductive than other host-guests and CX[4]-$TFSI^-$3 is less conductive than others. This information explains why the extremity of the $TFSI^-$4 (endo-cavity) forms a hydrogen bond with the cyclic group of the calixarene molecule. This system is very interesting in the optical and electrical fields. The energy gaps of these host-guests passing from CX[4]-T1 to CX[4]-T4 appear as a support to understand the active property of these molecules. It is very important that, the energy gaps are very high in the system or co-exists the H-binding between the cyclic net work of calixarene and the $TFSI^-$ion. Hence it is thermodynamically effective for the transfer of an electron to occur. The lowest value of the HOMO-LUMO+1 gap presented the transition from the ground to the first excited state of the CX[4]-$TFSI^-$3 complex. This transition is due to the weak transfer of conjugated electrons between these two molecules. We conclude that, this material has a low kinetic stability and chemical reactivity in comparison with other complexes. From to Figure 3, we deduce that, it exists an anti-bonding π character that has a maximum of electronic charges between the CX[4]-T4 and the calixarene molecule. The diagram of energy gap shows that these materials solve many problems in the optoelectronic field.

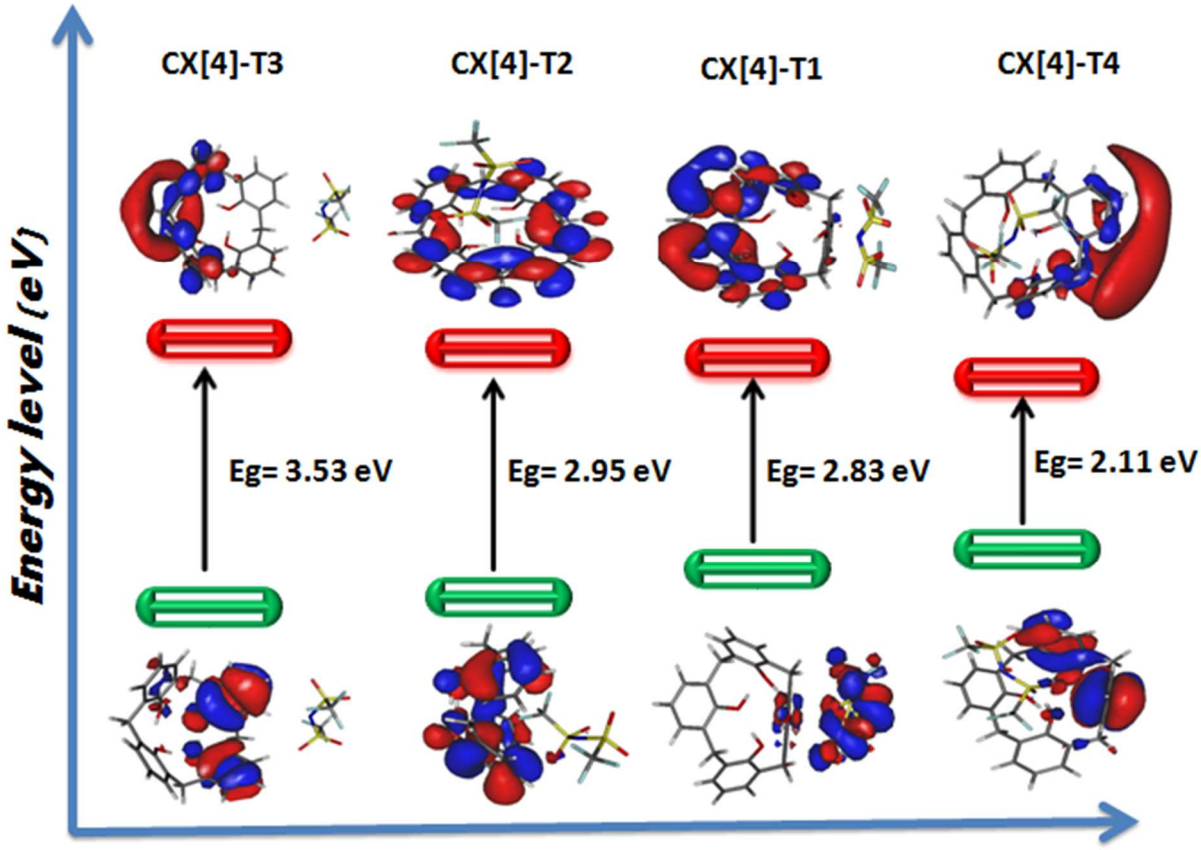

Figure 3. Frontier Molecular Orbital analysis of CX[4]-TFSI$^-$(CX[4]-T) complexes.

3.4. Charge NBO analysis

The charge NBO has been calculated to identify the characteristic of the charge transfer [34, 35] between the ionic molecule and the calix[4]arene material. The NBO charge calculation of the CX[4]-TFSI$^-$1/3 complex is equal to -0.978e$^-$. The Q_{NBO} of the CX[4]- TFSI$^-$2/4 chemical compounds is equal to -0.956e$^-$. In addition, the Q_{NBO} value of CX[4]-T1 and CX[4]-T3 inclusions explains the weak interaction between the guest and the host in this case. On the contrary, from Table 3, we find that the NBO loads of the supra-molecules complex CX[4]-T2/T4 is very important, which explains the strong interaction between the TFSI$^-$ and the calix[4]arene molecule. From Q_{NBO} calculation, we can clearly explain that, the TFSI$^-$ ion has a good stability in endo-cavity position of calixarene in comparison with exo-cavity position. We notice that always QNBO<0. This result shows that the transfer of charge always takes place from CX[4] to TFSI$^-$ ion.

Table 3: NBO charge analysis of CX[4]-$TFSI^-$ complexes

CX4-TFSI	Q_{NBO} (e^-)
CX4-$TFSI^-$ 1	-0.978
CX4-$TFSI^-$2	-0.956
CX4-$TFSI^-$3	-0.978
CX4-$TFSI^-$4	-0.956

3.5. NCI-RDG theory

The non covalent interaction (NCI) via reduced-density-gradient (RDG) facilitates the understanding of the nature of interactions in different types of encapsulated complexes. In this context, we have discovered the type of the interactions between the CX[4] and the $TFSI^-$ ion. The NCI isosurface for CX[4] and the specific encapsulated system ($TFSI^-$1, 2, 3 and 4) are shown in Figure 4. Moreover, the van der Waals interactions are shown with a green spot, the strong hydrogen bonding interactions are shown with a blue spot and the repulsive steric forces are visualized by the red spot. From Figure 4, we note that, the CX[4]-$TFSI^-$1 complex is characterized by the existence of the green spots located between the -S-H groups of the guest and the O-H groups of the host. The strong repulsive steric interactions are observed at the phenol five membered rings which are represented by the red spots. The strong H-bonding interactions have been conserved at the lower edge level. This existence of hydrogen bonds appears as blue spots (See Figure 4-a). In the case of the inclusion complex CX[4]-$TFSI^-$2, Figure 4-b explains that, the weak van der Waals type of attractive interactions co-exist in the area of the –C-F3 group interaction and the four symmetric phenol groups. There is also the appearance of the weak van der Waals bonds surrounding the CH_2 group of the calix[4]arene molecule. This type of attractive interactions is indicated by the green disk. In addition, it shows the appearance of the red spots in each phenol group center which explains the existence of the repulsion steric force in such zone. The existences of the weak intra-molecular hydrogen bonding interactions at the cyclic O…H net work are specified by the red spot. Concerning the CX[4]-$TFSI^-$3 complex, we found that the interaction between the $TFSI^-$ 3 ion and the calix[4]arene molecule is very weak, of van der Waals nature. The complex studied CX4-$TFSI^-$4 shows clearly that, the van der Waals type interactions (green disk) co-exist between the -S-O groups and the symmetrical phenol groups of the CX[4] molecule. Also, there is the formation of an attractive H-binding interaction (blue spot) between the guest and the host. The combination of the two types of interactions (van der Waals and H-binding) makes this complex more stable than the other host-guests. From Figure 4-d, we note

the existence of the weak hydrogen bonding interactions at the cyclic OH net work and repulsive steric forces at the four membered phenol ring.

The NCI iso-surface clearly explains that, the inclusion complex endo-cavity is more stable than the inclusion complex exo-cavity.

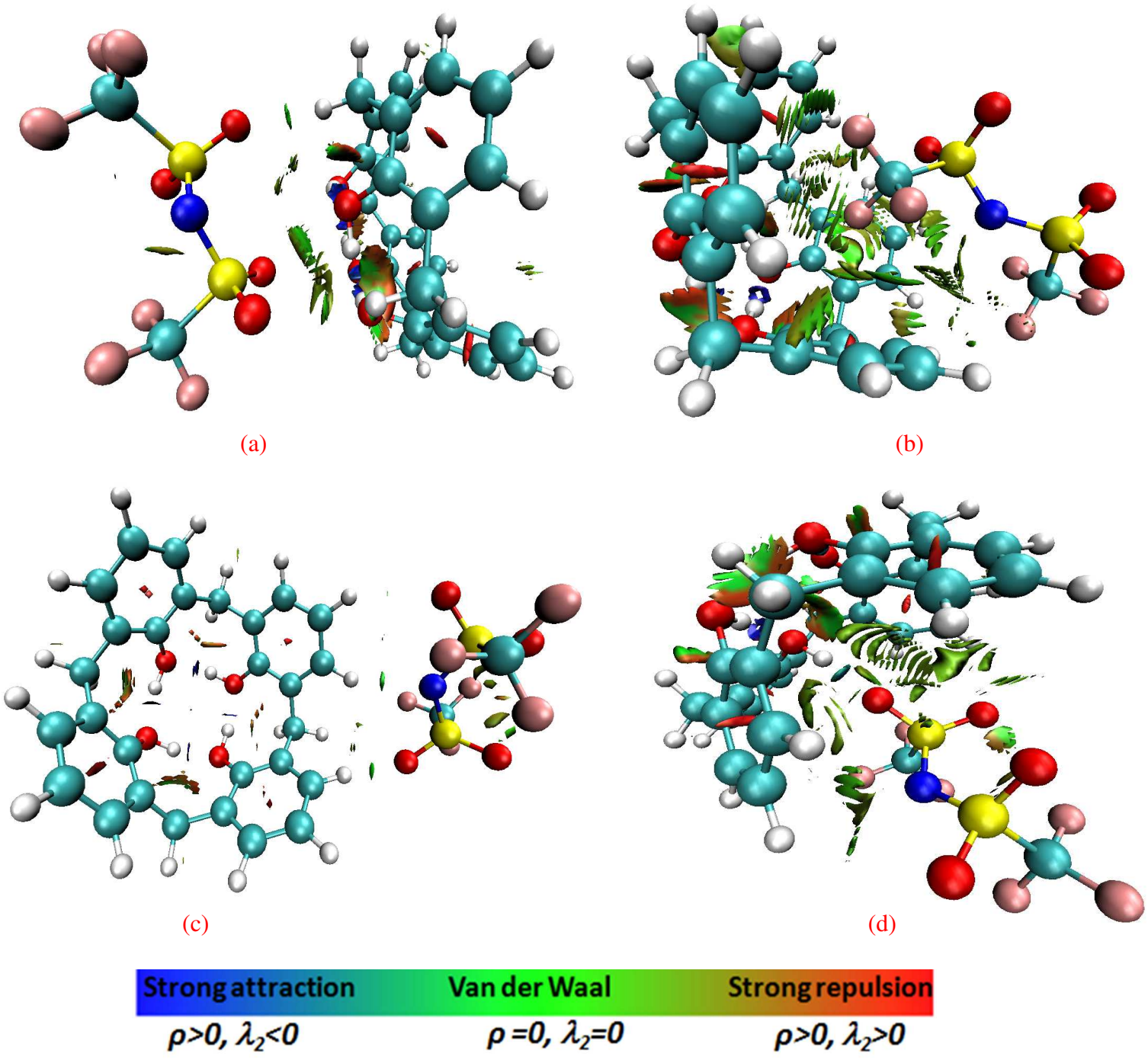

Figure 4. NCI isosurfaces for the inclusion complexes CX[4]-TFSI$^-$1 (a), CX[4]-TFSI$^-$2 (b), CX[4]-TFSI$^-$3 (c) and CX[4]-TFSI$^-$4 (d). The iso-surfaces were constructed with RGD = 0.5 au and the blue-red colors scaling from -0.01 to -0.01 au.

4. Conclusion

A DFT calculation of the binding energy of the CX4-$TFSI^-$ complexes show that the CX[4]-$TFSI^-$ (endo-cavity) interaction is the most stable system. The absorption spectra explain that the ionic material CX4-$TFSI^-$4 is a good candidate for the optoelectronic application. The NCI theory helps to discover the great, typical and the nature of the CX[4]-$TFSI^-$ interactions. This theory has demonstrated the great stability of the $TFSI^-$ (endo-cavity position) in comparison with $TFSI^-$ (exo-cavity position). The interrelation of this ion with the endo space of the cavity is explained by the strong bonds -SO-H (CX4- $TFSI^-$4) and -CF-H (CX4- $TFSI^-$2).

Acknowledgments

In this work, we were granted access to the HPC resources of the FLMSN, 'Fédération Lyonnaise de Modélisation et Sciences Numériques', partner of EQUIPEX EQUIP@MESO and to the 'Centre de calcul CC-IN2P3' at Villeurbanne, France.

Declarations

Author contribution statement

B. Gassoumi, H. Ghalla and R. Ben. Chaabane conceived, analyzed and interpreted the data.

They contributed to analysis tools, data and they participated in the writing of the article.

References

[1] M. Athar, M.Y. Lone, P.C. Jha, Recognition of anions using urea and thiourea substituted calixarenes: A density functional theory study of non-covalent interactions, Chemical Physics. 501 (2018) 68–77. doi:10.1016/j.chemphys.2017.12.002.

[2] S. Kumagai, K. Hayashi, T. Kameda, N. Morohashi, T. Hattori, T. Yoshioka, Identification of number and type of cations in water-soluble Cs+ and Na+ calix[4]arene-bis-crown-6 complexes by using ESI-TOF-MS, Chemosphere. 197 (2018) 181–184. doi:10.1016/j.chemosphere.2018.01.040.

[3] G. Arena, A. Contino, F.G. Gulino, A. Magrì, D. Sciotto, R. Ungaro, Complexation of small neutral organic molecules by water soluble calix[4]arenes, Tetrahedron Letters. 41 (2000) 9327–9330. doi:10.1016/S0040-4039(00)01687-7.

[4] A. Ortolan, I. Oestroem, G. Caramori, R. Parreira, A. Muñoz-Castro, F.M. Bickelhaupt, Anion Recognition by Organometallic Calixarenes: Analysis from Relativistic DFT Calculations, Organometallics. 37 (2018). doi:10.1021/acs.organomet.8b00292.

[5] B.J.C. Cabral, K. Coutinho, S. Canuto, Dynamics of endo- vs. exo-complexation and electronic absorption of calix[4]arene-Ar2, Chemical Physics Letters. 612 (2014) 266–272. doi:10.1016/j.cplett.2014.08.036.

[6] T. Haino, D.M. Rudkevich, A. Shivanyuk, K. Rissanen, J.R. Jr, Induced-Fit Molecular Recognition with Water-Soluble Cavitands, Chemistry – A European Journal. 6 (2000) 3797–3805. doi:10.1002/1521-3765(20001016)6:20<3797::AID-CHEM3797>3.0.CO;2-1.

[7] A. Wei, Calixarene-encapsulated nanoparticles: self-assembly into functional nanomaterials, Chem Commun (Camb). (2006) 1581–1591. doi:10.1039/b515806k.

[8] J.-F. Wang, L.-Y. Huang, J.-H. Bu, S.-Y. Li, S. Qin, Y.-W. Xu, J.-M. Liu, C.-Y. Su, A fluorescent calixarene-based dimeric capsule constructed via a M II –terpyridine interaction: cage structure, inclusion properties and drug release, RSC Advances. 8 (2018) 22530–22535. doi:10.1039/C8RA02146E.

[9] J.L. Atwood, G.A. Koutsantonis, C.L. Raston, Purification of C60 and C70 by selective complexation with calixarenes, Nature. 368 (1994) 229–231. doi:10.1038/368229a0.

[10] K.P. Aryal, H.K. Jeong, Functionalization of thermally reduced graphite oxide and carbon nanotubes by p-sulfonatocalix[4]arene and supramolecular recognition of tyrosine, Chemical Physics Letters. 714 (2019) 69–73. doi:10.1016/j.cplett.2018.10.074.

[11] S.A. Fahmy, F. Ponte, M.K. Abd El-Rahman, N. Russo, E. Sicilia, T. Shoeib, Investigation of the host-guest complexation between 4-sulfocalix[4]arene and nedaplatin for potential use in drug delivery, Spectrochimica Acta Part A: Molecular and Biomolecular Spectroscopy. 193 (2018) 528–536. doi:10.1016/j.saa.2017.12.070.

[12] D.T. Schühle, J.A. Peters, J. Schatz, Metal binding calixarenes with potential biomimetic and biomedical applications, Coordination Chemistry Reviews. 255 (2011) 2727–2745. doi:10.1016/j.ccr.2011.04.005.

[13] S. Balasaheb Nimse, T. Kim, Biological applications of functionalized calixarenes, Chemical Society Reviews. 42 (2013) 366–386. doi:10.1039/C2CS35233H.

[14] B. Hua, L. Shao, Z. Zhang, J. Sun, J. Yang, Pillar[6]arene/acridine orange host–guest complexes as colorimetric and fluorescence sensors for choline compounds and further application in monitoring enzymatic reactions, Sensors and Actuators B: Chemical. 255 (2018) 1430–1435. doi:10.1016/j.snb.2017.08.141.

[15] M. Athar, S. Das, P.C. Jha, A.M. Jha, Conformational equilibrium study of calix[4]tetrolarenes using Density Functional Theory (DFT) and Molecular Dynamics simulations, Supramolecular Chemistry. 30 (2018) 982–993. doi:10.1080/10610278.2018.1517876.

[16] K. Zare, N. Shadmani, E. Pournamdari, DFT/NBO study of Nanotube and Calixarene with anti-cancer drug, J Nanostruct Chem. 3 (2013) 75. doi:10.1186/2193-8865-3-75.

[17] S. Masoumi, E. Nadimi, F. Hossein-Babaei, Electronic properties of Ag-doped ZnO: DFT hybrid functional study, Phys. Chem. Chem. Phys. 20 (2018) 14688–14693. doi:10.1039/C8CP01578C.

[18] G. Mazzone, M.E. Alberto, F. Ponte, N. Russo, M. Toscano, Anion-π weak interactions in a heteroaromatic calixarene receptor. A theoretical investigation, Inorganica Chimica Acta. 470 (2018) 379–384. doi:10.1016/j.ica.2017.05.033.

[19] D. Senthilnathan, R.V. Solomon, S. Kiruthika, P. Venuvanalingam, M. Sundararajan, Are cucurbiturils better drug carriers for bent metallocenes? Insights from theory, J. Biol. Inorg. Chem. 23 (2018) 413–423. doi:10.1007/s00775-018-1547-7.

[20] G09 | Gaussian.com, http://gaussian.com/glossary/g09/

[21] Dennington RI, Keith T, Millam J, GaussView Version 5.0.8. Semichem Inc.

[22] S.F. Boys, F. Bernardi, The calculation of small molecular interactions by the differences of separate total energies. Some procedures with reduced errors, Molecular Physics. 19 (1970) 553–566. doi:10.1080/00268977000101561.

[23] E.R. Johnson, S. Keinan, P. Mori-Sánchez, J. Contreras-García, A.J. Cohen, W. Yang, Revealing Noncovalent Interactions, J. Am. Chem. Soc. 132 (2010) 6498–6506. doi:10.1021/ja100936w.

[24] S. Jeschke, P. Jankowski, A.S. Best, P. Johansson, Catching TFSI: A Computational-Experimental Approach to β-Cyclodextrin-Based Host-Guest Systems as electrolytes for Li-Ion Batteries, ChemSusChem. 11 (2018) 1942–1949 doi:10.1002/cssc.201800221

[25] N. Mchedlov-PetrossyanL, N.O.Vilkova, N.A. Vodolazkaya, A.G. Yakubovskaya, R.V. Rodik, V.I. Boyko, V.I. Kalchenko, The Nature of Aqueous Solutions of a Cationic Calix[4]arene: A Comparative Study of Dye–Calixarene and Dye–Surfactant Interactions, Sensors (Basel) 6 (2006) 962–977

[26] M. Israr, F. Faheem, F.T.Minhas, A. Rauf, S. Rauf, M.R. Shah, F. Rahim, K. Shah, M.I. Bhanger, Extraction Properties of Calix[4]arenes towards Sulphonated Dyes. American Journal of Analytical Chemistry 07 (2016) 219 doi:10.4236/ajac.2016.72019